BIOCHEMISTRY
including biophysical chemistry & molecular biology

Article

pubs.acs.org/biochemistry

Selective Mitogen Activated Protein Kinase Activity Sensors through the Application of Directionally Programmable D Domain Motifs

Laura B. Peterson,[†] Michael B. Yaffe,[‡] and Barbara Imperiali*,[†]

[†]Departments of Chemistry and Biology, and [‡]Departments of Biology and Biological Engineering, David H. Koch Institute for Integrative Cancer Research, Massachusetts Institute of Technology, Cambridge, Massachusetts 02139, United States

Supporting Information

ABSTRACT: Accurate and quantitative methods for measuring the dynamic fluctuations of protein kinase activities are critically needed as diagnostic tools and for the evaluation of kinase-targeted inhibitors, which represent a major therapeutic development area in the treatment of cancer and other diseases. In particular, rapid and economical methods that utilize simple instrumentation and provide quantitative data in a high throughput format will have the most impact on basic research in systems biology and medicine. There are over 500 protein kinases in the human kinome. Among these, the mitogen activated protein (MAP) kinases are recognized to be central players in key cellular signaling events and are associated with essential processes including growth, proliferation, differentiation, migration, and apoptosis. The major challenge with MAP kinase sensor development is achieving high selectivity since these kinases rely acutely on secondary interactions distal to the phosphorylation site to impart substrate specificity. Herein we describe the development and application of selective sensors for three MAP kinase subfamilies, ERK1/2, p38α/β, and JNK1/2/3. The new sensors are based on a modular design, which includes a sensing element that exploits a sulfonamido-oxine (Sox) fluorophore for reporting phosphorylation, a recognition and specificity element based on reported docking domain motifs and a variable linker, which can be engineered to optimize the intermodule distance and relative orientation. Following rigorous validation, the capabilities of the new sensors are exemplified through the quantitative analysis of the target MAP kinases in breast cancer progression in a cell culture model, which reveals a strong correlation between p38α/β activity and increased tumorgenicity.

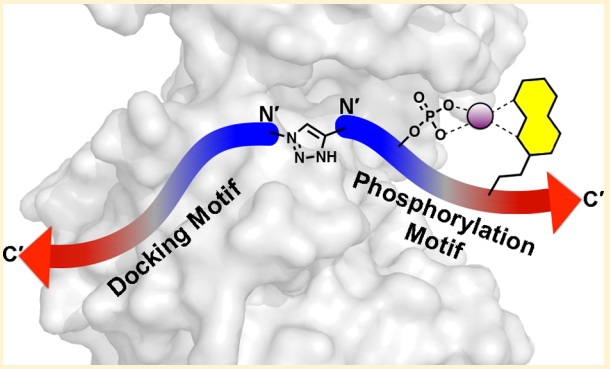

Protein phosphorylation on Ser, Thr, or Tyr is an abundant and ubiquitous post-translational modification (PTM) reaction. This PTM is central to all signaling pathways and impacts protein activity, interactions, localization, and degradation.[1,2] Defects in kinase signaling are implicated in many diseases, including cancer, and neurodegenerative and metabolic disorders.[3,4]

The mitogen activated protein (MAP) kinases are a family of related enzymes found at key nodes in major cell signaling pathways.[5] Each of the MAP kinase subfamilies is activated by different stimuli; ERK1/2 can be stimulated by growth factors, while the p38 and JNK subfamilies are typically stimulated by environmental stressors, such as DNA damage, heat shock, or oxidative stress.[6] Within each MAP kinase subfamily, each isoform often has overlapping roles, but differential activation may result from varying tissue distribution. These central kinases have been implicated in cancer, inflammatory, and other diseases and have thus become major drug discovery targets.[5,7,8] Because of their centrality in cellular function and frequent association with dysregulated cellular activity, individual MAP kinase subfamilies represent important targets for the development of quantitative activity sensors in order to understand the intricate dynamics of kinase activation and signaling networks at the systems levels.[5,7,8]

Commonly employed approaches for monitoring protein kinase activity include quantitative radioactivity-based approaches that rely on phosphoryl transfer from [γ-$^{32/33}$P]ATP to peptide or protein substrates, semiquantitative phosphoprotein-specific antibody-based methods, and mass spectrometry-based phosphoproteomics analyses.[9] In considering methods for direct and quantitative measurement of target kinase activities in the context of unfractionated cell lysates and tissue homogenates, radioactivity-based assays are not suitable due to the promiscuity of ATP in many cellular phosphorylation reactions. Alternatively, antibody-based measurements, while useful in cell and tissue lysates, are limited by the availability, reliability, and cost of specialized antibodies. Additionally, antibodies only provide a semiquantitative proxy for kinase activation, since assays are based on measuring the presence of phosphorylation that correlates with activated kinase—not the biochemical activity or

Received: July 11, 2014
Revised: August 22, 2014
Published: August 25, 2014

   dx.doi.org/10.1021/bi500862c | *Biochemistry* 2014, 53, 5771−5778

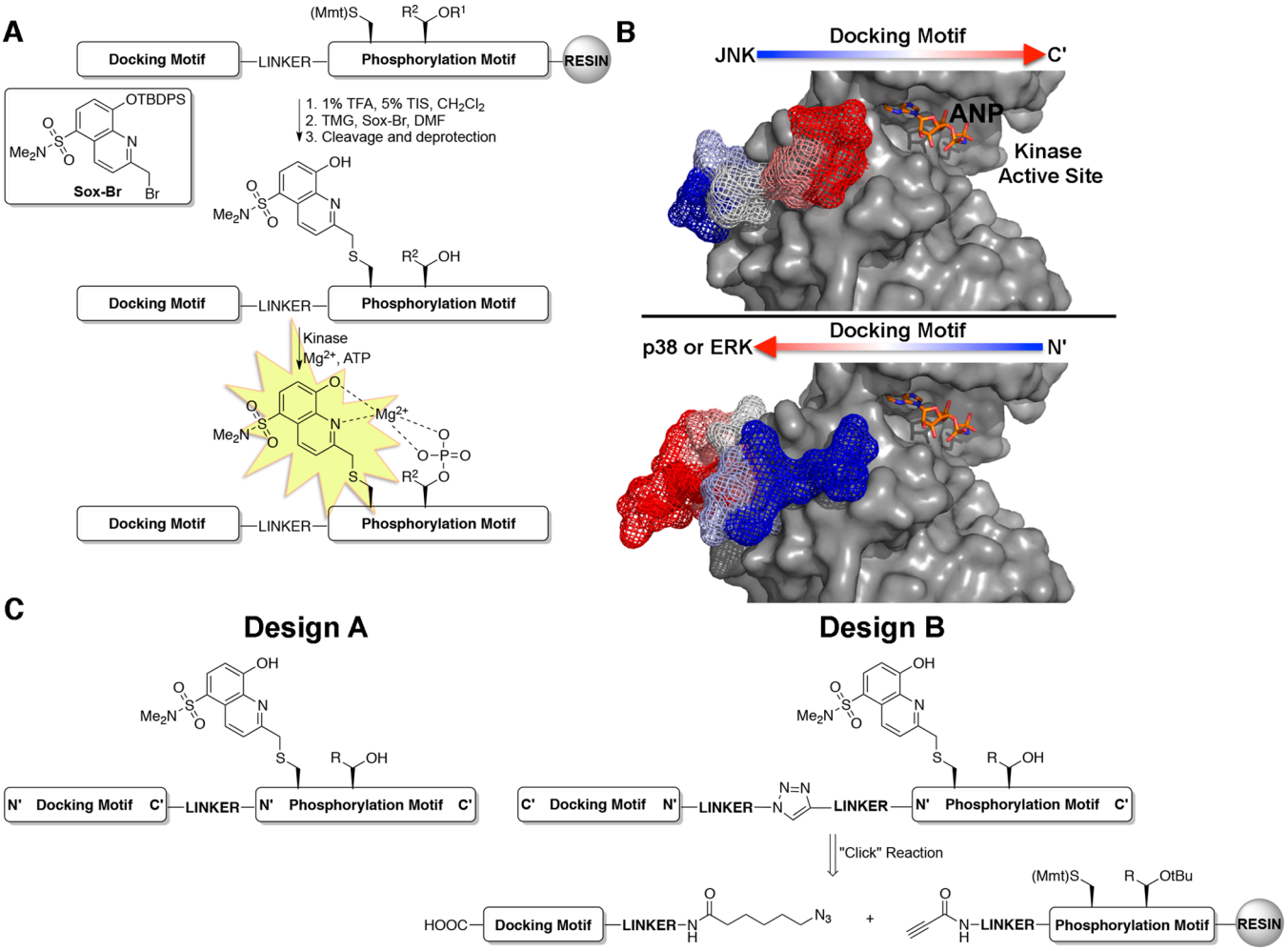

Figure 1. Design of MAP kinase activity sensors. (A) MAP kinase activity sensors are comprised of three domains: a docking motif to impart selectivity, a Sox-containing phosphorylation motif that provides fluorescence readout, and a linker between the two motifs (TMG = tetramethyl guanidine; R^1 = ^{t}Bu; R^2 = H or CH_3). (B) Co-crystal structures of JNK1 (top, gray surface) and p38α (bottom, gray surface) with substrate docking motifs, NFAT4 (mesh) and MK2 (mesh) respectively (PDB 2XS0[23] and 2OKR[41]). Arrows indicate the orientation that the docking motifs of each MAP kinase subfamily bind. The ATP derivative, phosphoaminophosphonic acid-adenylate ester (ANP), is shown in orange sticks for clarity. (C) Design strategies for MAP kinase activity sensors that have docking motifs in forward (Design A) and reversed (Design B) directions.

activation kinetics of the target kinase. Mass spectrometry-based methods, while also applicable in complex systems, require specialized training, instrumentation, and data analysis and are limited to semiquantitative analysis because data acquisition is labor- and equipment-intensive. In contrast, the application of fluorescence-based sensors that provide quantitative readouts of kinase activity have considerable potential to overcome these limitations,[10] provided that the challenges of sensor selectivity in complex mixtures can be adequately addressed.

We have previously reported protein kinase activity sensors that take advantage of the sulfonamido-oxine (Sox) fluorophore, which reports peptide phosphorylation via chelation-enhanced fluorescence (CHEF).[11−14] In these sensors, the CHEF fluorophore is introduced into peptide substrates via cysteine alkylation with the electrophilic 2-bromomethyl-5-(*N*,*N*′-dimethyl)sulfonamide-quinoline (Sox-Br) reagent, affording the CSox residue (Figure 1A). Generally, CSox is introduced into an optimized peptide substrate for a target kinase at positions ±2 or ±3 relative to the Ser/Thr/Tyr phosphorylation site. Using this small set of peptides, the best sensor is generally identified empirically based on the robustness of the fluorescence signal change and the substrate kinetic parameters. Typicallly, these 8−12 amino acid substrate sequences represent the major determinant of kinase specificity, i.e., the kinase consensus sequence.[15] The fluorescence-sensing mechanism is based on the chelate effect introduced by phosphorylation of the Ser/Thr/Tyr residue proximal to CSox, which enhances Mg^{2+} binding affinity compared to the unphosphorylated species and results in increased fluorescence due to the CHEF effect (Figure 1A). In this way, CSox-modified peptide substrates provide a means to directly measure kinase activity in continuous time-dependent assays in medium to high throughput (96−1536 well plate).

The MAP kinases present unique challenges in terms of sensor design due to the minimal consensus sequence for phosphorylation, which include either a Ser-Pro or Thr-Pro dipeptide motif.[16] As such motifs are common among MAP kinase substrates, an alternate strategy is required to realize selective sensors for specific kinases in the family. One way to achieve selectivity for the MAP kinases is to exploit docking grooves, or D-recruitment sites,[17] located distal to the enzyme active site that provide a second specificity-determining element.[18] Previous efforts in our laboratory took advantage of the ERK docking groove in the pursuit of an ERK1/2 sensor. The ERK1/2 sensor contained a CSox-based sensing module, which was ligated via

dx.doi.org/10.1021/bi500862c | *Biochemistry* 2014, 53, 5771−5778

native chemical ligation to the ERK1/2-selective PNT domain of the transcription factor Ets-1, a small protein domain that binds to the ERK1/2 docking groove.[13,19] However, while this approach afforded a sensor with advantageous kinetic parameters and fluorescence signaling properties, the semisynthetic strategy hampered sensor production and broad availability as the synthesis involved recombinant expression of the 100-residue PNT domain together with the preparation of a CSox peptide for native chemical ligation.

It was also realized that short docking motifs (8−12 amino acids) could also be incorporated into MAP kinase activity sensors without the need for a more extended protein domain such as the PNT domain.[19,20] MAP kinase docking sites generally feature an acidic cleft adjacent to a hydrophobic pocket and cognate substrates and upstream kinases include linear stretches of amino acids (docking/D-motifs, Figure 1B) that display complementary basic and hydrophobic features that bind the docking sites.[21−23] It has been observed through X-ray crystallography, by Garai and others, that these D-motifs can bind to MAP kinases in two opposite orientations.[23,24] More specifically, selective docking motifs for JNK1 were observed to bind in an N′ to C′ orientation, while selective docking motifs for ERK2 and p38α were observed to bind in an opposite, C′ to N′ orientation, relative to the enzyme active site (Figure 1B). Previous work showed that these D-motifs can be linked to CSox containing substrate peptides to provide selective sensors for certain MAP kinases.[13,19] One example resulted in a p38α sensor; however, the application of this sensor is hampered by crosstalk with other kinases in the context of cell lysates.[19] We therefore sought to expand this approach to other MAP kinases and create a general route to MAP kinase sensors. The optimization of each sensor was guided by their individual kinetic parameters, specifically the Michaelis constant (K_M) and k_{cat}. Critically, we note that sensors with advantageous K_M values allow for lower concentrations of sensor to be used in the assays, which makes phosphorylation of the CSox substrate by off-target kinases less problematic and as a consequence increases kinase selectivity in cell and tissue lysate based assays.

The design, synthesis, and evaluation of sensors for the MAP kinase subfamilies, p38α/β, ERK1/2, and JNK1/2/3, are described. The sensor design strategy exploits modular, peptide-based sensing and recognition elements, which are covalently assembled using an abiotic linker component that is tuned to optimize the distance between the modules and engineered to provide the optimal relative orientation of the recognition module relative to the sensing module. These MAP kinase sensors provide a means to quantify kinase activities in cell lysates over an extended time course and monitor kinase inhibitor activities in either recombinant or cell lysate-based assays. To underscore the utility of these MAP kinase subfamily selective sensors, we demonstrate their application in the analysis of breast cancer progression in a cell culture model, which reveals a correlation between p38α/β activity and increased tumorgenicity.

EXPERIMENTAL PROCEDURES

Peptide Synthesis and Characterization. Peptides were prepared using standard Fmoc-based solid-phase peptide synthesis as previously described.[12,19,25] The synthesis of peptides containing reversed docking domains is described in Supporting Information. Peptides were purified by preparative reversed-phase HPLC using dual wavelength detection (228 nm: amide; 360 nm: Sox). Peptide concentrations were then determined using UV−vis spectrophotometry based on the Sox-chromophore extinction coefficient of 8247 M^{-1} cm^{-1} at 355 nM in 0.1 M NaOH and 1 mM EDTA. Further peptide characterization is provided in the Supporting Information.

Recombinant Kinase Assays. All assays were performed in 96-well, 1/2 area, white, flat bottom plates at 30 °C in a BioTek Synergy H1 fluorescence plate reader. Reactions were carried out with sensors at varying concentrations (0.1−10 μM) in assay buffer containing 50 mM Tris, pH 7.4, 10 mM $MgCl_2$, 1 mM EGTA, 2 mM DTT, 0.01% Brij-35P, and 1 mM ATP at 30 °C and were initiated by addition of kinase. Kinase amounts used for each sensor are as follows: JNK1/2/3 20 ng/well; ERK1/2 10 ng/well; p38α/β 10 ng/well, and the kinases were added in kinase dilution buffer (20 mM Tris, pH 7.4, 0.01% Triton X-100, 0.1 mg/mL BSA, 1 mM DTT, 10% glycerol) at concentrations of 2−4 ng/μL (final volume/well = 120 μL). Following initiation of the kinase reaction, fluorescence was monitored over time (λ_{ex} = 360 nm; λ_{em} = 485 nm). Determination of kinetic parameters was performed as previously described.[12] Kinase panel screens were performed as described above with 15 nM of each indicated kinase while the sensor concentrations were held at 2 × K_M: JNK1/2/3 3 μM; p38α/β 1 μM; ERK1/2 2.5 μM. All kinases were purchased from Invitrogen.

Cell Culture and Lysis. HeLa cells were maintained in Dulbecco's Modified Eagle's Medium (DMEM, Invitrogen) supplemented with 10% fetal bovine serum (FBS, Atlanta Biological, Select Premium), 50 μg/mL streptomycin, and 50 U/mL penicillin. MCF10A and MCF10AT cells were maintained in complete HuMEC medium (per manufacturer instructions, Invitrogen) supplemented with 50 μg/mL streptomycin, and 50 U/mL penicillin. MCF10AT.KC12 and MCF10CA1 cells were maintained in advanced DMEM/F12 (1:1, Invitrogen) supplemented with 10% FBS, 50 μg/mL streptomycin, and 50 U/mL penicillin. All cells were cultured at 37 °C and 5% CO_2. HeLa cells were plated in 10 cm dishes in a density of 15 × 10^6 cells/dish on the day prior to the experiment and then treated with 1 μM anisomycin in DMSO (1% DMSO final concentration). To harvest cells at various times, they were washed with cold PBS, scraped from the plate in cold PBS, spun down and finally resuspended and lysed on ice for 15 min in 300 μL of lysis buffer containing 50 mM Tris, pH 7.4, 150 mM NaCl, 50 mM β-glycerophosphate, 10 mM sodium pyrophosphate, 1% Triton X-100, 2 mM EGTA, 1 mM DTT, protease inhibitor cocktail and phosphatase inhibitor cocktail. Lysates were then clarified via centrifugation (15 min × 14,000g) and protein concentration was determined via the BioRad colorimetric assay. Typical total protein concentrations of the lysates were 1,000−5,000 μg/mL. The MCF10 cell lines without anisomycin treatment were harvested in the same manner.

Kinase Assays in Cell Lysates. Assays were conducted using a concentration of 2 × K_M of the indicated sensor (3 μM JNK, 1 μM p38, 2.5 μM ERK, and 2.5 μM MK2) and 20 μg (for JNK) or 10 μg (for ERK, p38 or MK2) of total protein from cell lysates. Sensor solutions in assay buffer were prepared in bulk in buffer containing 50 mM Tris, 10 mM $MgCl_2$, 1 mM EGTA, 2 mM DTT, 0.01% Brij-35P, and 1 mM ATP (final assay concentrations) and aliquoted across 96-well plates. Reactions were initiated with addition of lysate (final volume/well = 120 μL), and fluorescence emission over time was monitored (at 30 °C; λ_{ex} = 360 nm; λ_{em} = 485 nm). Slopes representing the rates of phosphorylation were then determined by plotting fluorescence emission vs time data, and these values are reported as kinase activity.

dx.doi.org/10.1021/bi500862c | Biochemistry 2014, 53, 5771−5778

Table 1. Reported Docking Motifs and Corresponding Binding Affinities for Specific MAP Kinase[23]

			K_D (μM)			
kinase	docking motif	docking domain sequence	JNK	p38	ERK	orientation
JNK	NFAT4	ERPSRDHLYLPLEP	7.1	>100	>100	forward
p38	MK2	IKIKKIEDASNPLLLKRRKK	>100	0.05	19.5	reverse
ERK	RSK1	PQLKPIESSILAQRRVRKL	>100	0.3	23	reverse

Table 2. Sequences of Modular MAP Kinase Activity Sensors

Kinase	Docking Motif	Linker	Phosphorylation Site
JNK1/2/3	N'-ERPSRDHLYLPLEP-C'	PEG_2	N'-SANLLSP-**Csox**-PA-C'
p38α/β	C'-GKKRRKLLLPNSADEIKKIKI-N'	PEG_2-Triazole-PEG_2	N'-QP-**Csox**-ASPVV-C'
ERK1/2	C'-GLKRVRRQALISSEIPKLQP-N'	PEG_2-Triazole-PEG_2	N'-VP-**Csox**-LTPGGRR-C'

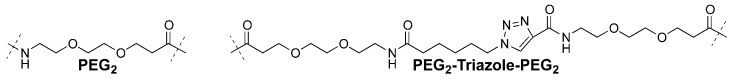

Western Blotting. Equal amounts of total protein (20 μg) were electrophoresed under reducing conditions (Bio-Rad Mini-Protean TGX, 4−15%), transferred to a nitrocellulose membrane, and immunoblotted with the corresponding phosphorylation site-specific antibodies (see Supporting Information). Membranes were then incubated with an appropriate IR-dye linked secondary antibody (Li-COR, IRDye 800CW goat antirabbit IgG and IRDye 680LT goat antimouse IgG) and visualized (Li-COR Odyssey IR-Scanner).

RESULTS AND DISCUSSION

Design and Synthesis of MAP Kinase Sensors. We envisioned chimeric MAP kinase sensors that contain a docking motif and CSox-containing phosphorylation site (Figure 1A). The CSox module would provide fluorescent readout of kinase activity in addition to a first layer of selectivity for the MAP kinase of interest based on the SP/TP and extended phosphorylation consensus sequence. The docking motif then provides a crucial secondary layer of selectivity for the MAP kinase of interest. Ideally, the phosphorylation motif and docking motif could be independently optimized and then joined by a linker to provide MAP kinase sensors. The choice of docking motif was guided by binding affinities between docking motif peptides with the kinase of interest. Using published dissociation constants (K_D) between various docking motifs and each of the MAP kinases, we chose docking motifs that manifested not only low micromolar K_D's, but also differential selectivity between each of the MAP kinases (Table 1).[23] An additional consideration in the choice of docking motif and subsequent sensor synthesis was the orientation in which the docking motif binds to its cognate MAP kinase-docking site. The docking motifs utilized in each of the three MAP kinases sensors are listed in Table 1, which shows that each manifested at least a 70-fold enhanced affinity for the MAP kinase subfamily of interest. The two alternate orientations of docking motifs led to two separate sensor designs (Design A and Design B), wherein those sensors with reversed docking motifs required an alternate synthetic strategy for preparation (Figure 1C, Design B). Synthesis of the JNK sensor, with a "forward" docking motif (Figure 1C, Design A) could be achieved via a continuous Fmoc-based solid phase peptide synthesis with incorporation of Fmoc-Cys(Mmt)-OH at the eventual site of CSox. The Sox fluorophore could then be installed as previously described.[12] The ERK and p38 sensors required a ligation between the N-termini of the phosphorylation site module that contained CSox and the docking motif, as is described below and in Supporting Information.

The CSox containing phosphorylation motifs were either empirically determined or guided by known substrate peptides of each kinase (Table 2). The CSox-containing phosphorylation motifs for ERK1/2 and p38α/β were previously determined,[13,19] while the JNK1/2/3 phosphorylation motif was based on a JNK1/2/3 phosphorylation site consensus sequence, namely, SANLLSPSPA.[26] The optimal CSox location in the JNK phosphorylation motif was determined by evaluating each of the peptides wherein CSox was placed at either the +2, +3, −2, or −3 positions. The phosphorylation-motif only peptide with CSox in the +2 position provided a 3.7-fold fluorescence increase upon phosphorylation, which translates into a useful Z' factor for kinase assays,[12] and this peptide manifested a Michaelis constant (K_M) of 52 ± 5 μM.

With the key modular elements established including a robust phosphorylation module and selective docking site module, the complete JNK1/2/3 sensor was developed after optimization of the linker between the two modules. Originally, we chose a native peptide linker between the docking motif and phosphorylation site, wherein we utilized either a two- or four-residue linker between the NFAT4-derived docking motif and the optimized phosphorylation motif. The amino acid linker was based on the JNK substrate, NFAT4, wherein we essentially extended the length of the docking domain, by either two (-SY-) or four (-SYRE-) residues. Following preparation of these two sensors, we evaluated their activity as JNK substrates. These two sensors showed modestly improved K_M values of 20 μM (2-residue) and 30 μM (4-residue), relative to the isolated phosphorylation site module. However, we reasoned that if both docking site and phosphorylation modules bound to JNK1/2/3 simultaneously, the complete sensors should manifest better K_M values than those that were observed. After careful consideration of the relative orientation of the docking motif to the ATP binding site (approximately 90°, Figure 1B), we reasoned that a flexible linker might allow for better simultaneous occupation of the docking groove and catalytic site. Toward this end, we chose a flexible polyethylene glycol (PEG) linker to join the two sensor modules. JNK sensors with a PEG_2 linker between the phosphorylation site and docking motif exhibited significantly improved kinetic parameters upon phosphorylation by JNK2 (K_M = 0.95 ± 0.13 μM). This Michaelis constant was within the target range (low micromolar) that we proposed would provide selectivity for the MAP kinase of interest in cell lysate based assays.

dx.doi.org/10.1021/bi500862c | Biochemistry 2014, 53, 5771−5778

Table 3. Kinetic Parameters for Each MAP Kinase Activity Sensor

sensor	isoform	K_M (μM)	V_{max} (μmol min^{-1} mg^{-1})	k_{cat} (min^{-1})	catalytic efficiency (min^{-1} μM^{-1})
JNK1/2/3	JNK1	3.30 ± 1.1	0.38 ± 0.05	17.9 ± 2.2	5.4
	JNK2	0.95 ± 0.13	0.37 ± 0.02	18.2 ± 1.3	19.2
	JNK3	2.84 ± 1.3	0.35 ± 0.07	26.6 ± 5.6	9.4
ERK1/2	ERK1	1.14 ± 0.02	0.42 ± 0.03	29.9 ± 2.0	26.2
	ERK2	1.15 ± 0.18	0.90 ± 0.01	62.8 ± 0.7	54.6
p38α/β	p38α	0.31 ± 0.03	1.37 ± 0.08	92.6 ± 5.4	298.7
	p38β	0.14 ± 0.03	0.84 ± 0.13	39.6 ± 6.3	282.9

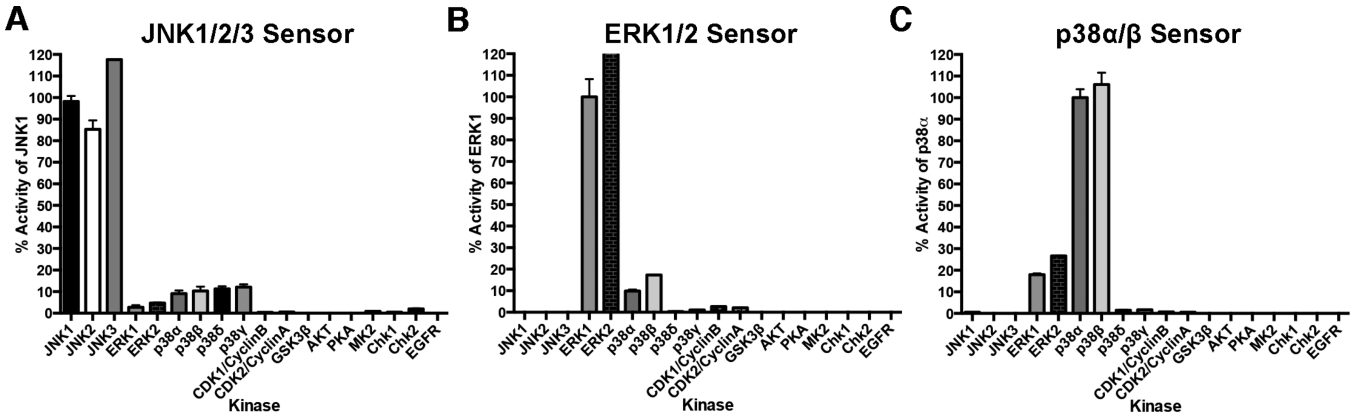

Figure 2. MAP kinase activity sensors can selectively report kinase activity in recombinant assays. (A–C) Kinase selectivity profile for each sensor was determined by evaluating kinase activity in a panel of related kinases (15 nM kinase, 2 × K_M sensor concentration). Values are plotted as a percentage of the target kinase.

In order to explore the generality of the approach, we sought to expand this modular chemical strategy, including a flexible linker, to prepare sensors for ERK1/2 and p38α/β. However, as it was proposed that reversed docking motifs were required for selective p38α/β and ERK1/2 sensors, a complementary synthetic strategy was required to facilitate a formal N-terminus to N-terminus ligation, between the phosphorylation/sensing site and the docking motif modules (Figure 1C, Design B). To achieve this, the two modules were independently synthesized and following capping with 6-azidohexanoic acid (azide) and propiolic acid (alkyne), respectively, the modules were conjugated via a Copper-mediated "click" reaction (Supporting Information).[27] This ligation allowed for effective incorporation of reversed docking motifs into MAP kinase activity sensors. Following the preparation of docking-domain based activity sensors for ERK1/2, p38α/β, and JNK1/2/3 (Table 2), the ability to function as kinase activity sensors was investigated.

MAP Kinase Sensors Robustly and Selectively Report Kinase Activity. Each sensor was validated and characterized by determining the kinetic parameters of phosphorylation (Table 3 and Supplementary Figure 1, Supporting Information). All three MAP kinase sensors manifested improved Michaelis constants (K_M) as compared to previously reported sensors.[13,19] This reduction in K_M enables improved selectivity in complex cell lysates systems, as the concentration used in assays is directly related to the K_M. Following the validation and kinetic characterization of each sensor with the appropriate recombinantly expressed and activated MAP kinase, each sensor was screened against a panel of related and nonrelated kinases to evaluate sensor selectivity (Figure 2A–C). The JNK sensor reported activity for each of the three major JNK isoforms, JNK1, JNK2, and JNK3, while the selectivity for JNK1/2/3 over other MAP and non-MAP kinases was excellent at concentrations of 2 × K_M, with no greater than 12.5% activity observed for any of the off target kinases. Interestingly, the activities (and K_M's) observed for each of the JNK isoforms correlated well with the sequence homology among the three isoforms; i.e., the JNK sensor had similar catalytic efficiency between JNK1 and JNK3, which show the highest homology to each other and slightly lower efficiency for JNK2 (Table 4 and Supplementary Figures 2–5, Supporting Information). The p38 sensor demonstrated robust selectivity for the highly similar p38 isoforms, p38α and p38β, over the other p38 isoforms (p38δ and p38γ), as well as over ERK1/2, JNK1/2/3, and other non-MAP kinases evaluated. Lastly, the ERK sensor selectively reported ERK1 and ERK2 activity, with measurable crosstalk observed with p38α and p38β (10% and 17%). However, this p38α/β crosstalk will only be relevant in situations where the relative amounts of ERK and p38 are similar.

Table 4. Amino Acid Sequence Homologies within Each MAP Kinase Subfamily

	p38α	p38β	p38δ	p38γ
p38α		73	61	64
p38β	88		61	64
p38δ	76	79		67
p38γ	80	80	80	

	JNK1	JNK2	JNK3
JNK1		81	91
JNK2	89		84
JNK3	95	91	

	ERK1	ERK2
ERK1		88
ERK2	94	

Identities (%)

Similarity (%)

dx.doi.org/10.1021/bi500862c | Biochemistry 2014, 53, 5771–5778

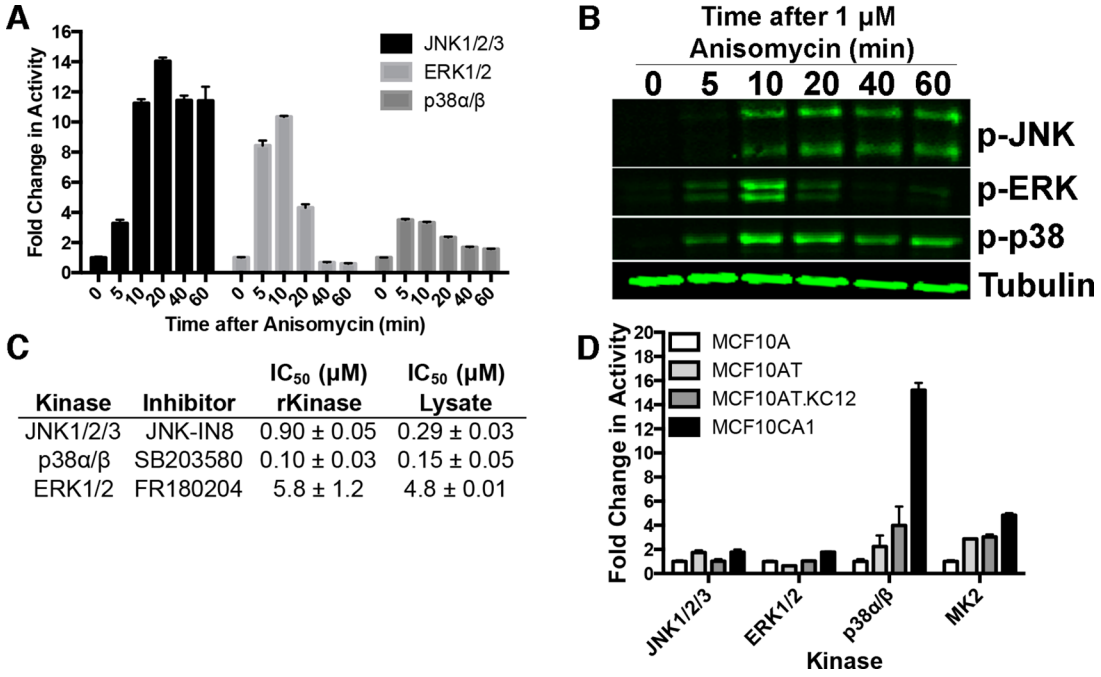

C

Kinase	Inhibitor	IC_{50} (μM) rKinase	IC_{50} (μM) Lysate
JNK1/2/3	JNK-IN8	0.90 ± 0.05	0.29 ± 0.03
p38α/β	SB203580	0.10 ± 0.03	0.15 ± 0.05
ERK1/2	FR180204	5.8 ± 1.2	4.8 ± 0.01

Figure 3. MAP kinase activities can be monitored in cell lysates. (A) Activity of JNK1/2/3, ERK1/2, and p38α/β in HeLa cell lysates following treatment with 1 μM anisomycin. Values are plotted as a fold change from the 0 min control and are representative of triplicate measurements performed in duplicate. (B) Western blot analysis of the same anisomycin treated lysates as A. Tubulin is shown as a loading control. (C) MAP kinase activity sensors can report inhibitor activities in cell lysates or with recombinant kinases (rKinase). (D) MAP kinase and MK2 activities were monitored in MCF10 cell line series. Values are shown as fold change from level in MCF10A cell line. Values are representative of triplicate measurements performed in duplicate.

In one example, we observed that p38 activity was not detected in cell lysates using the ERK sensor (Supplementary Figure 6, Supporting Information). In addition, given the broad availability of selective p38 inhibitors, such as SB203580, the p38 crosstalk can be minimized by running a control assay that includes a selective p38α/β inhibitor (Supplementary Figure 7, Supporting Information). Importantly, none of the MAP kinase sensors were phosphorylated by the cyclin dependent kinases (CDK1/Cyclin B and CDK2/Cyclin A), which are closely related proline-directed kinases. In the event that the small amount of crosstalk observed between the MAP kinase subfamilies would hamper activity measurements in complex mixtures, selective kinase inhibitors could be employed to minimize this effect. Following promising results using purified, activated enzymes, we sought to investigate the utility of these sensors in unfractionated cell lysates.

MAP Kinase Sensors Report Kinase Activity in Unfractionated Cell Lysates. To first assess the ability of each sensor to report kinase activity in cell lysates, HeLa cells were treated with anisomycin, a known stimulator of the stress response and potent activator of the three major MAP kinases. The cells were then lysed and kinase activity measurements were made (Figure 3A,B). ERK1/2, p38α/β, and JNK1/2/3 each gave a different activation profile, both temporally and in maximal activation, following treatment with anisomycin. In parallel, Western blot analysis for the phospho-MAP kinases was performed. Results obtained using the Sox-based activity sensors correlated well with traditional Western blot analysis. One notable difference between the two methods is in detecting and quantifying low basal kinase activities. The kinase activity sensors report low basal activities, in situations where signals for the active phosphokinases could not be observed without maximizing the intensity settings, which compromises the resolution of the other signals.

The kinase selectivity in cell lysates was determined by performing kinase activity measurements in anisomycin-treated lysates in the presence of selective inhibitors for each of the MAP kinase subfamilies. The half maximal inhibitory concentration (IC_{50}) for each kinase inhibitor-kinase pair was evaluated against both recombinant kinase and in anisomycin treated lysates. By comparing the relative IC_{50} values in lysates vs recombinant kinase and the remaining kinase activity at the highest inhibitor concentration, the kinase selectivity can be inferred. For all three kinase sensors evaluated, the IC_{50} in cell lysates is consistent with the values derived from assays with recombinant kinases (Figure 3C and Supplementary Figure 8, Supporting Information). In the case of the JNK inhibitor, JNK-IN8, a lower IC_{50} was observed in cell lysates. This could be due to the selectivity of the compound for the various JNK isoforms.[28] In addition, the residual activity detected at the highest inhibitor concentrations used for each of the MAP kinases was approximately 10% or less. This correlates well with the kinase selectivity observed in the kinase panel selectivity screen (Figure 2A–C). Overall, these results demonstrate the utility of Sox-based kinase activity sensors in monitoring kinase activity following various stimuli.

Profiling MAP Kinase Activity in a Cellular Model of Breast Cancer Progression. We next sought to apply these sensors to evaluate MAP kinase signaling in a cell culture model of breast cancer progression. We chose the MCF10A series, which is a set of isogenic cell lines that represent progression of proliferative disease,[29] as a system to explore whether the MAP kinase sensors could be used to provide quantitative data which may correlate with the cancer progression phenotype. Until now, a quantitative analysis of the activities of the MAP kinases in this system has not been reported. Specifically, we used the MCF10A,

dx.doi.org/10.1021/bi500862c | Biochemistry 2014, 53, 5771−5778

MCF10AT, MCF10AT1K.c12, and the MCF10CA1h cell lines. MCF10A cells represent benign, normal breast epithelium.[30] Initially transformed MCF10AT cells have been transfected with oncogenic H-ras,[31] premalignant MCF10ATK.c12 cells were isolated after xenograft passage of MCF10AT cells,[29,32] and fully malignant MCF10CA1h cells were isolated after further xenograft passages in mice.[33] Previously, mRNA gene expression profiling, copy number variation analysis, and proteomic analysis have been performed in this series of cell lines.[34−36] Although these studies provided useful information, mRNA expression and protein levels may vary with enzymatic activity, and we were therefore interested in changes in MAP kinase activities during the course of disease progression (Figure 3D).

We monitored ERK1/2, JNK1/2/3, and p38α/β activity as well as MAP kinase activated protein 2 (MAPKAP2, MK2), which is a downstream target of p38α/β and is involved in the DNA damage response and other stress and inflammatory pathways.[12,37,38] As shown in Figure 3D, the activities of ERK1/2 and JNK1/2/3 do not significantly change in the varying MCF10A cell lines. Strikingly, we observed significantly higher activity of p38α/β in MCF10AT, MCF10AT.Kc12, and MCF10CA1 (2.2-, 4.0-, and 15.2-fold, respectively), compared to the benign MCF10A cells. Presumably, this increased activity of p38α/β leads to the increased activity observed with MK2, as MK2 is a substrate of p38α/β. Also of interest is in the comparison of the gene expression and proteomic analysis of these cell lines. Neither study identified p38 or MK2 as having increased levels,[34−36] demonstrating that kinase activity measurements can provide valuable insight into cellular signaling that would not have been otherwise observed in genome/proteome wide experiments. The current study demonstrates the utility of quantitative kinase activity sensors in probing kinase activities in various biological contexts, potentially providing insights into interesting biological questions.

Herein we have detailed the design and characterization of selective MAP kinase activity sensors using a docking domain based strategy. We chose docking domains for p38α/β, ERK1/2, and JNK1/2/3 that bound preferentially to the kinase of interest. When introduced into chimeric sensors, the docking motifs imparted selectivity for each intended kinase. Interestingly, the docking motifs for ERK1/2 and p38α/β bound in an opposite orientation as compared to JNK1/2/3 and required an alternative synthetic strategy that allowed for N-terminus to N-terminus ligation between the docking motif and phosphorylation domain. Using recombinant kinase panel screens, we demonstrated that each sensor was selective for the intended kinase and furthermore this selectivity translated into selectivity in cell lysates. With this set of kinase sensors, we proceeded to profile MAP kinase activities in different cellular contexts. In this regard, we were interested in MAP kinase activities in neoplastic disease and investigated MAP kinase activities in the MCF10A model of breast cancer progression. Through this study, we observed that p38 activity was significantly increased in each successive cell line, while p38 activity was 15-fold higher in the most aggressive MCF10CA1h cell line as compared to the benign MCF10A cell line. These studies demonstrated the utility of kinase activity sensors in profiling kinase activities in various contexts.

Overall, these sensors demonstrate the utility of using secondary kinase interactions in combination with Sox-containing phosphorylation motifs, to generate useful kinase activity sensors. Future investigation of isoform selective MAP kinase activity sensors or use of the current sensors with isoform selective inhibitors would further enhance the information that can be garnered from these sensors. In addition, the use of kinase activity sensors may provide different insights and/or novel perspectives into different biological phenomenon as compared to other methods including gene profiling and proteomic analysis. We anticipate that these sensors will be extremely valuable reagents for systems biology studies of signaling.[39] Furthermore, the combination of these three sensors that can distinguish and rigorously quantify kinase activities through the three main MAP kinase signaling pathways represents a major advance for the signaling community. For example, we and others have shown that accurate measurements of these pathways alone is sufficient to predict the apoptotic response to cytokine and growth factor combination treatments.[40] These sensors may also provide valuable tools in profiling kinase activities in clinical tumor samples. In conclusion, we have prepared a useful set of tools for selectively monitoring MAP kinase activities that are useful in quantifying disease progression in cell culture models of disease and in diseased tissues.

■ ASSOCIATED CONTENT

Supporting Information

Synthetic procedures, peptide characterizations, and expanded methods section. This material is available free of charge via the Internet at http://pubs.acs.org.

■ AUTHOR INFORMATION

Corresponding Author

*E-mail: imper@mit.edu; phone: 1-617-253-1838.

Funding

This project was supported by the Integrated Cancer Biology Program at MIT (NIH U54-CA112967 − PI Douglas A. Lauffenburger and M.B.Y.), the NIH (GM104047 and ES015339 - M.B.Y.), and a Koch Institute Bridge Project Grant (M.B.Y. and B.I.). L.B.P. was supported by an NIH Ruth L. Kirschstein National Research Service Award (F32 GM102992).

Notes

The authors declare the following competing financial interest(s): Imperiali, Shults and Lukovic hold a patent on the CSox methodology.

■ ACKNOWLEDGMENTS

We acknowledge Nathanael Gray for the generous gift of the JNK-selective inhibitor, JNK-IN8, and Professor Lee Bardwell for advice regarding a JNK substrate peptide.

■ ABBREVIATIONS

MAP, mitogen activated protein; K_D, dissociation constant; K_M, Michaelis constant; IC_{50}, half maximal inhibitory concentration; CHEF, chelation-enhanced fluorescence; Sox, sulfonamido oxine; Sox-Br, 2-bromomethyl-5-(*N*,*N*′-dimethyl)-sulfonamidoquinoline

■ REFERENCES

(1) Endicott, J. A., Noble, M. E. M., and Johnson, L. N. (2012) The structural basis for control of eukaryotic protein kinases. *Annu. Rev. Biochem. 81*, 587−613.

(2) Manning, G., Whyte, D. B., Martinez, R., Hunter, T., and Sudarsanam, S. (2002) The protein kinase complement of the human genome. *Science 298*, 1912−1934.

(3) Blume-Jensen, P., and Hunter, T. (2001) Oncogenic kinase signalling. *Nature 411*, 355−365.

(4) Lahiry, P., Torkamani, A., Schork, N. J., and Hegele, R. A. (2010) Kinase mutations in human disease: interpreting genotype-phenotype relationships. *Nat. Rev. Genet. 11*, 60−74.
(5) Lawrence, M. C., Jivan, A., Shao, C., Duan, L., Goad, D., Zaganjor, E., Osborne, J., McGlynn, K., Stippec, S., Earnest, S., Chen, W., and Cobb, M. H. (2008) The roles of MAPKs in disease. *Cell Res. 18*, 436−442.
(6) Cargnello, M., and Roux, P. P. (2011) Activation and Function of the MAPKs and Their Substrates, the MAPK-Activated Protein Kinases. *Microbiol. Mol. Biol. Rev. 75*, 50−83.
(7) Dhillon, A. S., Hagan, S., Rath, O., Kolch, W. MAP kinase signalling pathways in cancer. *Oncogene 26*, 3279−3290.
(8) Kyriakis, J. M., and Avruch, J. (2012) Mammalian MAPK Signal Transduction Pathways Activated by Stress and Inflammation: A 10-Year Update. *Physiol. Rev. 92*, 689−737.
(9) Johnson, S. A., and Hunter, T. (2005) Kinomics: methods for deciphering the kinome. *Nat. Methods 2*, 17−25.
(10) Rothman, D. M., Shults, M. D., and Imperiali, B. (2005) Chemical approaches for investigating phosphorylation in signal transduction networks. *Trends Cell Biol. 15*, 502−510.
(11) Shults, M. D., Carrico-Moniz, D., and Imperiali, B. (2006) Optimal Sox-based fluorescent chemosensor design for serine/threonine protein kinases. *Anal. Biochem. 352*, 198−207.
(12) Luković, E., González-Vera, J. A., and Imperiali, B. (2008) Recognition-Domain focused chemosensors: Versatile and efficient reporters of protein kinase activity. *J. Am. Chem. Soc. 130*, 12821−12827.
(13) Luković, E., Vogel Taylor, E., and Imperiali, B. (2009) Monitoring protein kinases in cellular media with highly selective chimeric reporters. *Angew. Chem., Int. Ed. 121*, 6960−6963.
(14) González-Vera, J. A., Luković, E., and Imperiali, B. (2009) A rapid method for generation of selective Sox-based chemosensors of Ser/Thr kinases using combinatorial peptide libraries. *Bioorg. Med. Chem. Lett. 19*, 1258−1260.
(15) Ubersax, J. A., and Ferrell, J. E., Jr. (2007) Mechanisms of specificity in protein phosphorylation. *Nat. Rev. Mol. Cell Biol. 8*, 530−541.
(16) Bardwell, L. (2006) Mechanisms of MAPK signalling specificity. *Biochem. Soc. Trans. 34*, 837−841.
(17) Abramczyk, O., Rainey, M. A., Barnes, R., Martin, L., and Dalby, K. N. (2007) Expanding the Repertoire of an ERK2 Recruitment Site: Cysteine Footprinting Identifies the D-Recruitment Site as a Mediator of Ets-1 Binding. *Biochemistry 46*, 9174−9186.
(18) Sharrocks, A. D., Yang, S.-H., and Galanis, A. (2000) Docking domains and substrate-specificity determination for MAP kinases. *Trends Biochem. Sci. 25*, 448−453.
(19) Stains, C. I., Luković, E., and Imperiali, B. (2010) A p38α-Selective chemosensor for use in unfractionated cell lysates. *ACS Chem. Biol. 6*, 101−105.
(20) Fernandes, N., Bailey, D. E., VanVranken, D. L., and Allbritton, N. L. (2007) Use of docking peptides to design modular substrates with high efficiency for mitogen-activated protein kinase extracellular signal-regulated kinase. *ACS Chem. Biol. 2*, 665−673.
(21) Barsyte-Lovejoy, D., Galanis, A., and Sharrocks, A. D. (2002) Specificity determinants in MAPK signaling to transcription factors. *J. Biol. Chem. 277*, 9896−9903.
(22) Bardwell, A. J., Frankson, E., and Bardwell, L. (2009) Selectivity of Docking Sites in MAPK Kinases. *J. Biol. Chem. 284*, 13165−13173.
(23) Garai, A., Zeke, A., Gogl, G., Toro, I., Fordos, F., Blankenburg, H., Barkai, T., Varga, J., Alexa, A., Emig, D., Albrecht, M., and Reményi, A. (2012) Specificity of linear motifs that bind to a common mitogen-activated protein kinase docking groove. *Science Signaling 5*, ra74.
(24) Smith, J. A., Poteet-Smith, C. E., Lannigan, D. A., Freed, T. A., Zoltoski, A. J., and Sturgill, T. W. (2000) Creation of a Stress-activated p90 Ribosomal S6 Kinase: The carboxyl-terminal tail of the MAPK-activated protein kinases dictates the signal transduction pathway in which they function. *J. Biol. Chem. 275*, 31588−31593.
(25) Shults, M. D., Janes, K. A., Lauffenburger, D. A., and Imperiali, B. (2005) A multiplexed homogeneous fluorescence-based assay for protein kinase activity in cell lysates. *Nat. Methods 2*, 277−284.
(26) Bogoyevitch, M. A., and Kobe, B. (2006) Uses for JNK: the many and varied substrates of the c-Jun N-terminal kinases. *Microbiol. Mol. Biol. Rev. 70*, 1061−1095.
(27) Tornoe, C. W., Christensen, C., and Meldal, M. (2002) Peptidotriazoles on solid phase: [1,2,3]-triazoles by regiospecific copper(i)-catalyzed 1,3-dipolar cycloadditions of terminal alkynes to azides. *J. Org. Chem. 67*, 3057−3064.
(28) Zhang, T., Inesta-Vaquera, F., Niepel, M., Zhang, J., Ficarro, S. B., Machleidt, T., Xie, T., Marto, J. A., Kim, N., Sim, T., Laughlin, J. D., Park, H., LoGrasso, P. V., Patricelli, M., Nomanbhoy, T. K., Sorger, P. K., Alessi, D. R., and Gray, N. S. (2012) Discovery of potent and selective covalent inhibitors of JNK. *Chem. Biol. 19*, 140−154.
(29) Dawson, P. J., Wolman, S. R., Tait, L., Heppner, G. H., and Miller, F. R. (1996) MCF10AT: a model for the evolution of cancer from proliferative breast disease. *Am. J. Pathol. 148*, 313−319.
(30) Soule, H. D., Maloney, T. M., Wolman, S. R., Peterson, W. D. J., Brenz, R., McGrath, C. M., Russo, J., Pauley, R. J., Jones, R. F., and Brooks, S. C. (1990) Isolation and characterization of a spontaneously immortalized human breast epithelial cell line, MCF-10. *Cancer Res. 50*, 6075−6086.
(31) Basolo, F., Elliott, J., Tait, L., Chen, X. Q., Maloney, T., Russo, I. H., Pauley, R., Momiki, S., Caamano, J., and Klein-Szanto, A. J. (1991) Transformation of human breast epithelial cells by c-Ha-ras oncogene. *Mol. Carcinog. 4*, 25−35.
(32) Miller, F. R., Soule, H. D., Tait, L., Pauley, R. J., Wolman, S. R., Dawson, P. J., and Heppner, G. H. (1993) Xenograft model of progressive human proliferative breast disease. *J. Natl. Cancer Inst. 85*, 1725−1732.
(33) Santner, S. J., Dawson, P. J., Tait, L., Soule, H. D., Eliason, J., Mohamed, A. N., Wolman, S. R., Heppner, G. H., and Miller, F. R. (2001) Malignant MCF10CA1 cell lines derived from premalignant human breast epithelial MCF10AT cells. *Breast Cancer Res. Treat. 65*, 101−110.
(34) Rhee, D. K., Park, S. H., and Jang, Y. K. (2008) Molecular signatures associated with transformation and progression to breast cancer in the isogenic MCF10 model. *Genomics 92*, 419−428.
(35) Kadota, M., Yang, H. H., Gomez, B., Sato, M., Clifford, R. J., Meerzaman, D., Dunn, B. K., Wakefield, L. M., and Lee, M. P. (2010) Delineating Genetic Alterations for Tumor Progression in the MCF10A Series of Breast Cancer Cell Lines. *PLoS One 5*, e9201.
(36) Choong, L. Y., Lim, S., Chong, P. K., Wong, C. Y., Shah, N., and Lim, Y. P. (2010) Proteome-wide profiling of the MCF10AT breast cancer progression model. *PLoS One 5*, e11030.
(37) Reinhardt, H. C., and Yaffe, M. B. (2009) Kinases that control the cell cycle in response to DNA damage: Chk1, Chk2, and MK2. *Curr. Opin. Cell Biol. 21*, 245−255.
(38) Kyriakis, J. M., and Avruch, J. (2001) Mammalian mitogen-activated protein kinase signal transduction pathways activated by stress and inflammation. *Physiol. Rev. 81*, 807−869.
(39) Lee, M. J., Ye, A. S., Gardino, A. K., Heijink, A. M., Sorger, P. K., MacBeath, G., and Yaffe, M. B. (2012) Sequential Application of Anticancer Drugs Enhances Cell Death by Rewiring Apoptotic Signaling Networks. *Cell 149*, 780−794.
(40) Janes, K. A., Reinhardt, H. C., and Yaffe, M. B. (2008) Cytokine-Induced signaling networks prioritize dynamic range over signal strength. *Cell 135*, 343−354.
(41) Haar, E. T., Prabakhar, P., Liu, X., and Lepre, C. (2007) Crystal Structure of the P38α-MAPKAP Kinase 2 Heterodimer. *J. Biol. Chem. 282*, 9733−9739.